

# Electron attachment and electron ionization of acetic acid clusters embedded in helium nanodroplets

F. Ferreira da Silva,<sup>ab</sup> S. Jaksch,<sup>a</sup> G. Martins,<sup>b</sup> H. M. Dang,<sup>c</sup> M. Dampc,<sup>d</sup>  
S. Deniff,<sup>a</sup> T. D. Märk,<sup>a</sup> P. Limão-Vieira,<sup>b</sup> J. Liu,<sup>e</sup> S. Yang,<sup>e</sup> A. M. Ellis<sup>e</sup> and  
P. Scheier<sup>\*a</sup>

Received 3rd September 2009, Accepted 2nd October 2009

First published as an Advance Article on the web 6th November 2009

DOI: 10.1039/b918210a

The effect of incident electrons on acetic acid clusters is explored for the first time. The acetic acid clusters are formed inside liquid helium nanodroplets and both cationic and anionic products ejected into the gas phase are detected by mass spectrometry. The cation chemistry (induced by electron ionization at 100 eV) is dominated by production of protonated acetic acid (Ac) clusters,  $\text{Ac}_n\text{H}^+$ , although some fragmentation is also observed. In the case of anion production (at 2.8 eV electron energy) there is a clear distinction between the monomer and the clusters. For the monomer the dominant product is the dehydrogenated species,  $[\text{Ac}-\text{H}]^-$ , whereas for the clusters both the parent anion,  $\text{Ac}_n^-$ , and the dehydrogenated species,  $[\text{Ac}_n-\text{H}]^-$ , have similar abundances. A particularly intriguing contrast between the monomer and cluster anions is that helium atoms are seen attached to the latter whereas no evidence of helium atom attachment is found for the monomer. This surprising observation is attributed to the formation of acyclic (head-to-tail) acetic acid clusters in helium nanodroplets, which have more favourable electronic properties for binding helium atoms. The acyclic clusters represent a local minimum on the potential energy surface and in the case of the dimer this is distinct from the cyclic isomer (the global minimum) identified in gas phase experiments.

## 1. Introduction

The interaction of electrons with molecules is important for understanding processes arising from radiation-induced chemistry.<sup>1</sup> Low energy electrons can trigger chemical reactions and it has been well established that the interaction of ionizing radiation with matter generates secondary electrons with energies below 30 eV.<sup>2</sup> It has recently been demonstrated that these secondary electrons may induce single and double strand breaks in supercoiled DNA.<sup>3</sup> Carboxylic acids are relevant to this important problem because their functionality is common to all amino acids. Consequently, the response to electron damage is an important component in gaining an understanding of how biological systems are affected by low energy electrons.

Acetic acid,  $\text{CH}_3\text{COOH}$ , is the second simplest organic acid after formic acid ( $\text{HCOOH}$ ). In order to assess its intrinsic response to low-energy electrons, it is useful to carry out experiments in an environment where other molecules are

absent. Dissociative electron attachment to acetic acid monomer in the gas phase was first reported by Sailer *et al.*<sup>4</sup> Electrons in the energy range 0–13 eV led to the formation of nine fragment anions, with the dominant products assigned to  $\text{CH}_3\text{COO}^-$ ,  $(\text{CH}_2\text{O}_2)^-$  and  $(\text{HCOO})^-$ . The anions are generated by two low energy resonances at 0.75 and 1.5 eV. Subsequent work by Pelc *et al.* has explored these low energy resonances at higher resolution, providing evidence for vibrational structure in the attachment spectra.<sup>5</sup> The only other electron attachment study relevant to the current work is the investigation of chemical reactions in clusters of trifluoroacetic acid triggered by electrons at sub-excitation energies ( $<2$  eV). This work, by Langer *et al.*,<sup>6</sup> showed that intracluster dissociative electron attachment leads to solvated fragment ions with remarkable size selectivity, *i.e.* only dimers respond.

In contrast to the anions, there have been several studies of the cations produced by electron ionization of acetic acid clusters. The first such investigation was reported by Sievert *et al.*,<sup>7</sup> but subsequent work by Lifshitz and Feng<sup>8</sup> and Pithawalla *et al.*<sup>9</sup> have also addressed this topic.

In this paper we continue our recently instigated series of studies of the interaction of electrons with molecules and clusters in helium nanodroplets.<sup>10–16</sup> Here the ion chemistry takes place in a cold environment dictated by the extremely low temperature (0.38 K) of the surrounding liquid helium. In the present study we report on the findings of both electron attachment and electron ionization measurements on helium nanodroplets doped with acetic acid molecules. Included in this work is the first observation of dissociative electron

<sup>a</sup> Institut für Ionenphysik und Angewandte Physik and Center of Molecular Biosciences Innsbruck, Universität Innsbruck, Technikerstr. 25, A-6020 Innsbruck, Austria.

E-mail: Paul.Scheier@uibk.ac.at

<sup>b</sup> Atomic and Molecular Collisions Laboratory, CEFITEC, Departamento de Física, Universidade Nova de Lisboa, 2829-516 Caparica, Portugal

<sup>c</sup> Atomic and Physics KVI, Zernikelaan 25 NL-9747 AA Groningen, The Netherlands

<sup>d</sup> Department of Physics of Electronic Phenomena, Gdansk University of Technology, 80-952, Gdansk, Poland

<sup>e</sup> Department of Chemistry, University of Leicester, Leicester, UK LE1 7RH

attachment to acetic acid clusters. We also present evidence, based on the observation of helium atoms attached to the cluster anions, for the formation of metastable acyclic (head-to-tail) acetic acid clusters in the low temperature environment provided by liquid helium rather than the cyclic clusters seen in the gas phase.

## 2. Experimental

The experimental measurements were carried out using a double focusing mass spectrometer coupled with a helium cluster source. The apparatus and basic operating procedure has already been described elsewhere, so only a brief account will be given here.<sup>16–18</sup> The helium nanodroplets are formed by supersonic expansion at high pressure (20 bar) with high purity gaseous helium (>99.9999%). Before expansion the helium passes through a liquid nitrogen-cooled trap, which helps to remove any remaining trace impurities. The nozzle tip consists of a platinum disk (Günther Frey GmbH & Co. KG, Berlin) with a 5  $\mu\text{m}$  diameter and is cooled to 11 K using a closed-cycle cryostat. Under these operating conditions we expect helium droplets with an average size of  $10^4$  helium atoms to be produced.<sup>19,20</sup> The pressure in the cluster source chamber is around  $10^{-2}$  Pa.

The expanding flow of helium droplets is skimmed 10 mm downstream of the nozzle and then passes into another vacuum chamber, where the doping with acetic acid takes place. Controlled addition of acetic acid is achieved *via* a needle valve, with a typical partial pressure of  $1.5 \times 10^{-3}$  Pa in the pick-up cell. Subsequently, the beam of helium droplets passes through a second skimmer and into the source region of a mass spectrometer (maintained at a pressure of  $7 \times 10^{-6}$  Pa). The ion source is of the Nier-type with an energy resolution of  $\sim 1$  eV. The current is set to 100  $\mu\text{A}$  and 20  $\mu\text{A}$  for positive and negative mass scans, respectively. The mass spectrometer is a modified two-sector field instrument (Varian-MAT CH5), which provides a mass resolution of  $\Delta m/m$  200 with open slits. All signal intensities in the mass spectra presented in this paper are measured as ion counts per second and are expressed in Hz.

The sample of normal acetic acid was obtained from Riedel-de Hen (99–100%). Some experiments were also carried out with partially deuterated acetic acid ( $\text{CH}_3\text{COOD}$ ), which was purchased from Sigma Aldrich (99.99%). Prior to use both liquids were subjected to several freeze-pump-thaw cycles in order to remove any dissolved atmospheric gases.

## 3. Results and discussion

### 3.1 Positive ion mass spectra

Fig. 1 presents the mass spectrum of positive ions formed by electron ionization of acetic acid clusters embedded in helium droplets. The scan range extends up to 1000 Thomson (Th) and peaks are observed corresponding to cluster ions containing up to 16 acetic acid monomer units. In addition, a series of closely spaced (4 Th separation) peaks are seen in the low mass part of the spectrum and are due to helium cluster ions,  $\text{He}_n^+$ . Charged dopant species are thought to be formed in helium droplets after the initial ionization of a helium atom

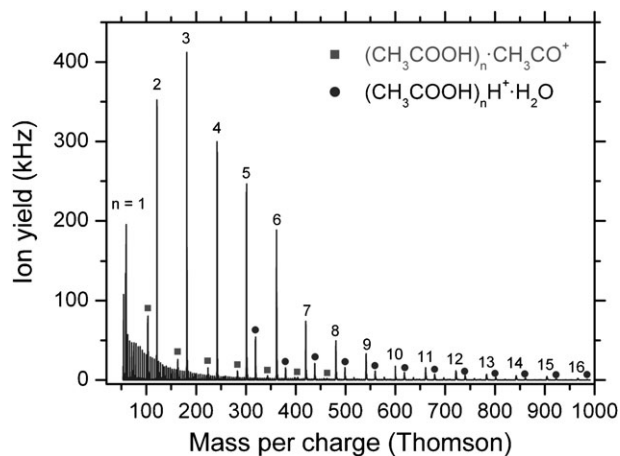


**Fig. 1** Positive ion mass spectrum of  $\text{CH}_3\text{COOH}$  measured at 100 eV electron energy. The peaks labelled with numbers indicate the corresponding protonated cluster ions  $(\text{CH}_3\text{COOH})_n\text{H}^+$ .

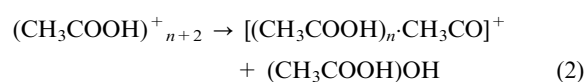
( $\text{IE}(\text{He}) = 24.59$  eV) near the surface or in the interior of the droplet.<sup>21</sup> The resulting  $\text{He}^+$  migrates through the cluster by resonant charge transfer and the migration process terminates either by charge transfer to the dopant species or by the formation of  $\text{He}_n^+$ . Charge transfer to the dopant inevitably transfers over a considerable amount of energy, since the first ionization energies of organic molecules are typically very much less than that of atomic helium. Consequently, the degree of dissipation of this excess energy by the surrounding helium is a critical factor in determining the reaction products that are ejected into the gas phase. With a droplet size of  $10^4$  helium atoms and assuming that each evaporated helium atom can remove  $\sim 5$   $\text{cm}^{-1}$  of energy,<sup>19</sup> a helium droplet of average size can dissipate up to  $5 \times 10^4$   $\text{cm}^{-1}$ , or  $\sim 6.2$  eV. In practice the actual quantity will be somewhat smaller due to evaporative loss of helium as molecules are added to the droplets.

The most intense series of peaks arises from the protonated parent clusters, *i.e.*  $(\text{CH}_3\text{COOH})_n\text{H}^+$ . These ions have been observed previously in electron ionization studies of acetic acid clusters<sup>7</sup> and are thought to be formed by loss of H atoms from the carboxylic acid groups after initial ionization, as shown in reaction (1) below:

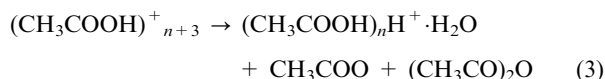


In principle the reactant on the left hand side of reaction (1) might also survive because of the intense cooling potential of the helium droplets. However, there is no evidence for the production of any of these unprotonated acetic acid cluster cations in the current experiments.

Two other significant reaction products are observed. For clusters up to  $n = 7$ , an adduct ion composed of the acetic acid cluster and a  $\text{CH}_3\text{CO}$  fragment is clearly visible. These ions are not easily seen for larger clusters, although this may simply be due to the declining cluster ion intensity. These ions have also been reported previously and the reaction proposed by Sievert *et al.* is:<sup>7</sup>



The other significant products are clusters of the type  $(\text{CH}_3\text{COOH})_n\text{H}^+\cdot\text{H}_2\text{O}$ , which appear with detectable intensities only for  $n \geq 5$ . Once again this observation ties in with previous gas phase work, where the specific cluster ion  $(\text{CH}_3\text{COOH})_5\text{H}^+\cdot\text{H}_2\text{O}$  has been reported to be a 'magic' cluster.<sup>8,9</sup> In that earlier work these hydronium-containing clusters were generated when a small amount of water was deliberately added to the gaseous sample. However, in the current experiments no water was added. Of course it is possible that traces of water vapour, *e.g.* from residual water adsorbed on the wall of the vacuum chamber or the inlet line, enter the helium droplets. However, an alternative possibility is that these clusters are generated by the following reaction:



To see if this is plausible, mass spectra from deuterated acetic acid in helium nanodroplets have also been recorded. To reduce the possibility of H/D exchange in the inlet line, the sample inlet was charged and degassed with deuterated acetic acid several times and was subjected to several freeze-pump-thaw cycles. Fig. 2 shows a positive ion mass scan recorded by electron ionization at 100 eV for  $\text{CH}_3\text{COOD}$  in helium droplets. The experimental conditions were similar to those employed for the undeuterated acetic acid experiments. The assignment of spectral features is essentially the same as in the previous section. Once again, protonated acetic acid-water clusters begin to be observed at the acetic acid pentamer. However, this time the cluster peaks are found at 20 mass units above the  $(\text{CH}_3\text{COOD})_n\text{D}^+$  peaks, which is consistent with an assignment to  $(\text{CH}_3\text{COOD})_n\text{D}^+\cdot\text{D}_2\text{O}$ . This shows that the water comes from within the original acetic acid clusters, indicating that reaction (3) is the main source of  $(\text{CH}_3\text{COOD})_n\text{D}^+\cdot\text{D}_2\text{O}$  in helium nanodroplets, in contrast to the gas phase work mentioned earlier.

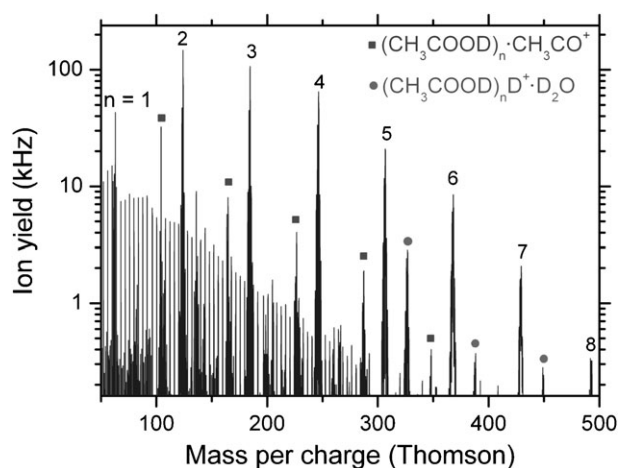


**Fig. 2** Positive ion mass spectrum of  $\text{CH}_3\text{COOD}$  measured at 100 eV electron energy. The peaks labelled with numbers indicate the corresponding deuterated cluster ions  $(\text{CH}_3\text{COOD})_n\text{D}^+$ .

### 3.2 Negative ion mass spectra for $(\text{CH}_3\text{COOH})_n$

Fig. 3 shows a negative ion mass scan between 50 and 190 Th obtained by attachment of electrons at 2.8 eV to helium droplets doped with acetic acid. The most prominent peaks in Fig. 3 correspond to the negatively charged dimer (120 Th) and trimer (180 Th). Slightly weaker are the dehydrogenated dimer and trimer anions at 119 and 179 Th, respectively. Interestingly, the monomer shows only the dehydrogenated anion.

The observation of only the dehydrogenated parent monomer anion is identical with previous gas phase studies of electron attachment to acetic acid. However, there have been no prior studies of electron attachment to acetic acid clusters so it is not immediately clear whether the survival of the parent anions for the dimer and trimer is a special feature of electron attachment in helium droplets, and in particular the potential for rapid cooling of excited anions, or whether it is a consequence of the presence of additional acetic acid unit(s). Langer *et al.* have reported electron attachment to the trifluoroacetic acid (TFA) monomer and its clusters in the gas phase.<sup>6</sup> Both parent and dehydrogenated anions are seen for monomeric TFA, so acetic acid is clearly different and the question of the role of the liquid helium in the formation of parent cluster anions is therefore not answered by this comparison and it remains an open question.

In the gas phase low energy electron attachment to acetic acid monomer can lead not only to H atom loss from the carboxylic acid group, but also ejection of  $\text{CH}_2$ .<sup>4</sup> The maximum probability for ejection of  $\text{CH}_2$  in the gas phase occurs at an electron energy of 0.75 eV, whereas loss of H from the carboxylic acid group peaks at roughly 1.5 eV. These excitation energies will be shifted to significantly higher energies for acetic acid in helium droplets for reasons discussed in section 3.4. In the gas phase the ejection of H is only marginally more probable than the loss of  $\text{CH}_2$ . However, for acetic acid clusters in helium nanodroplets the  $\text{CH}_2$  loss channel seems to

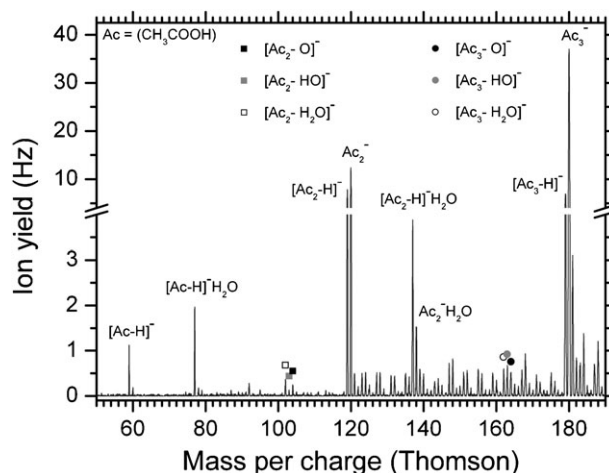


**Fig. 3** Negative ion mass spectrum of  $\text{CH}_3\text{COOH}$  measured at 2.8 eV electron energy. Although not explicitly labelled in the figure, the long series of peaks above 120 Th arising from addition of helium atoms to the dimer and trimer anions (both parent and dehydrogenated) should be noted. Clusters with up to 14 helium atoms have been identified for the acetic acid dimer anion.

be completely absent, which is a remarkable change in chemistry. It has been seen previously that the surrounding liquid helium can hinder the formation of reactions which proceed *via* 'loose' transition states<sup>22</sup> and this may be the reason why the methylene ejection channel is not observed for acetic acid and its clusters. Furthermore, CH<sub>2</sub> loss requires considerable structural rearrangement, *i.e.* H transfer from the methyl group to the carboxylic acid group. In recent studies we could demonstrate that He droplets efficiently quench decay reactions that require time consuming rearrangement processes by rapid energy transfer from the excited dopant to the surrounding superfluid He matrix.<sup>23,24</sup>

Another substantial set of peaks arises from the dehydrogenated parent anions with an attached H<sub>2</sub>O molecule. In the case of the clusters the hydrated parent anion is also observed. In order to confirm the source of the water, additional experiments with deuterated acetic acid were carried out. Fig. 4 shows a scan recorded at 2.8 eV electron energy in the mass range between 200 and 260 Th. At the lower masses it is possible to assign the peak at 203 Th as the hydrated form of the trimer anion, while the 201 peak is the same species but with loss of D. A substantial part (0.9 Hz) of the peak at mass 202 can be assigned to the isotopomer of 201 containing one <sup>13</sup>C and the remaining part is a combination of a He solvated anion (~0.6 Hz) and a trimer clustered with HDO (1 Hz), due to some residual H/D exchange.

Additionally, the peaks at 204 and 224 are consistent with the formation of acetic anhydride. This has precedent since the corresponding anhydride has been reported by Langer *et al.* in the case of electron attachment to trifluoroacetic acid clusters.<sup>6</sup> The signal at mass 204 corresponds to the dimer of acetic anhydride (see reaction (4) below) while mass 224 corresponds to one molecule of acetic anhydride coupled with two molecules of deuterated acetic acid, as per reaction (5) below:

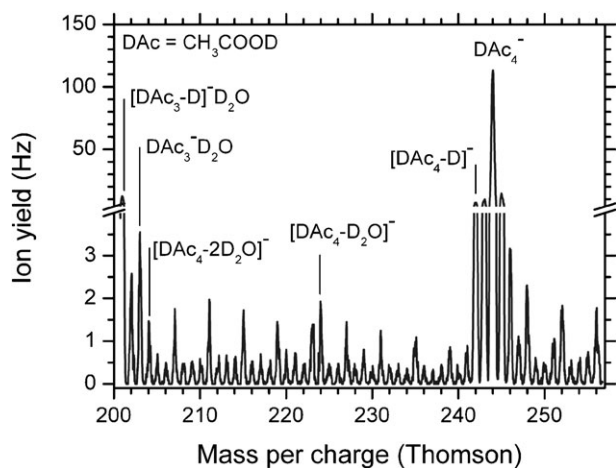
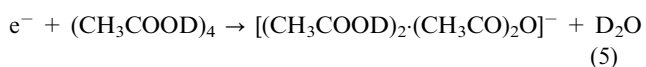
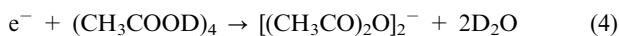
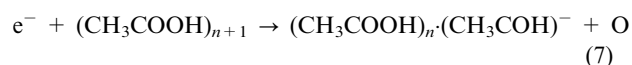
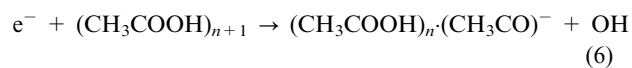


Fig. 4 Part of the negative ion mass spectrum of CH<sub>3</sub>COOD measured at 2.8 eV electron energy.

The peaks at 242 and 244 are assigned to the tetramer with loss of one D atom and the undissociated tetramer, respectively.

Other low intensity peaks in Fig. 3 can be assigned to the dimer and trimer ions having lost O or OH, where we propose the reactions:



The analogous reactions for TFA clusters were not reported by Langer *et al.*<sup>6</sup>

### 3.3 Anions with attached helium atoms

Previous studies of anions ejected from helium nanodroplets have shown that some anions leave with one or more helium atoms attached.<sup>23,25–28</sup> However, a surprising observation in the current work is that only the dimer anions and larger clusters show any evidence of attached helium atoms, as will be evident from inspection of Fig. 3. Consequently, there is something unique about the monomer which prevents attachment of helium atoms or which releases the helium atoms before the aggregated clusters can reach the detector.

Helium atoms are likely to be rapidly ejected from the anion if the temperature is too high since the binding will be very weak. Although the dominant product for the monomer is the dehydrogenated species rather than the parent anion, added helium atoms are seen for both parent and dehydrogenated dimers and larger clusters. There is no reason to expect a substantially larger heat release for the monomer anion formation when compared to the clusters and consequently there is no reason to expect the temperature of the monomer anion to be significantly higher than that of the cluster anions. As a result, we rule out excessive heat released as the reason why helium atoms are not attached to the monomer species.

A more likely explanation stems from the structure and electronic properties of the anions. One of the unique features of helium nanodroplets is that the rapid and continuous cooling has the potential to trap species in shallow minima reached through favourable long-range interactions. In the case of carboxylic acids, the long range electrostatic forces will favour a head-to-tail alignment of the molecules to maximise the dipole–dipole interaction. On the other hand, at least for small clusters, the global minimum on the potential energy surface is known to be a closed structure which maximises the hydrogen bonding. In the case of the dimers this gives rise to a cyclic structure composed of two hydrogen bonds. For the dimers of formic and acetic acid, the cyclic structures are the only isomers detected in gas phase work.<sup>29–33</sup> Evidence that helium nanodroplets trap the dimers in the acyclic (head-to-tail) structure has recently come from an infrared spectroscopic study of formic acid dimers.<sup>34</sup> There is also prior evidence from formic acid monomers in argon matrices that the acyclic structure is a precursor to the cyclic structure as the matrix is annealed.<sup>35</sup> Most recently of all, comprehensive *ab initio* molecular dynamics calculations have been carried out on formic acid dimer formation.<sup>36</sup> These support the notion that the head-to-tail isomer dominates, although the



calculations also find that other isomers, including the global minimum structure, are also present at low temperatures. Given the clear evidence in the case of formic acid, a similar scenario should pertain for acetic acid. Thus it seems highly likely that acyclic structures dominate for acetic acid clusters in helium nanodroplets.

We speculate that this acyclic structure confers favourable electronic properties to bind helium atoms. One possibility is the formation of the monomer anion resulting in a relatively uniform negative charge distribution which is unfavourable for attachment of helium atoms. The dimer and larger clusters may see the negative charge localized on one of the monomer units (particularly in the case of dehydrogenated cluster anions), leaving the other free to undergo more attractive interactions with helium atoms. An alternative mechanism is that the helium atoms bind through interaction with the electric dipole moment of the anion. Although the dipole moments of neither acetic acid monomer anion nor the cluster anions have been determined, values for the neutral species are known. The dipole moment for acetic acid monomer is known accurately (1.6741(10) D<sup>37</sup>) and calculated values exist for the various conformers of the dimer.<sup>38</sup> The cyclic dimer has a zero dipole moment, whereas the acyclic isomer has an estimated value of 3.95 D. Assuming this marked difference in dipole moments is maintained in the anions, then it is conceivable that binding through the dipole plays a key role. Of course this is currently speculation and it would be valuable to explore the binding mechanism of the helium atoms to acetic acid monomer and cluster anions through detailed *ab initio* calculations. It is hoped that this work will stimulate such an investigation.

### 3.4 Anion efficiency curves

Fig. 5 and 6 illustrate how the yields of parent and dehydrogenated parent cluster anions vary with incident electron energy. Fig. 5 is for the trimer of acetic acid and is dominated by a low energy resonance peaking at approximately 3.5 eV. As mentioned earlier, in gas phase acetic acid there are two low energy reaction channels, one leading to CH<sub>2</sub> loss and the other leading to H atom loss. The cross sections for these two processes were found to be similar, but their peak energies were different (0.75 eV for CH<sub>2</sub> ejection and 1.5 eV for H atom loss). Although CH<sub>2</sub> ejection is not observed in the current work, it seems likely that both of these resonant features contribute to the low energy peak in Fig. 5 and we observe merely a superposition of the two which cannot be distinguished at the current electron energy resolution. The peak maximum is shifted to higher energies than in the gas phase because of the energy required for the electron to penetrate inside the helium droplet.<sup>17,23</sup> The peak at approximately 22 eV corresponds to the same excitation process but in combination with inelastic scattering (auto-scavenging) of the electron by a helium atom (electronic excitation to the 2<sup>3</sup>S state at 19.82 eV above the ground electronic state).

Fig. 6 shows the efficiency curve for formation of the dehydrogenated acetic acid dimer anion. Here the strongest peak is a broad feature centred near 10 eV. This is indicative of higher energy resonances that lead to fragmentation of the

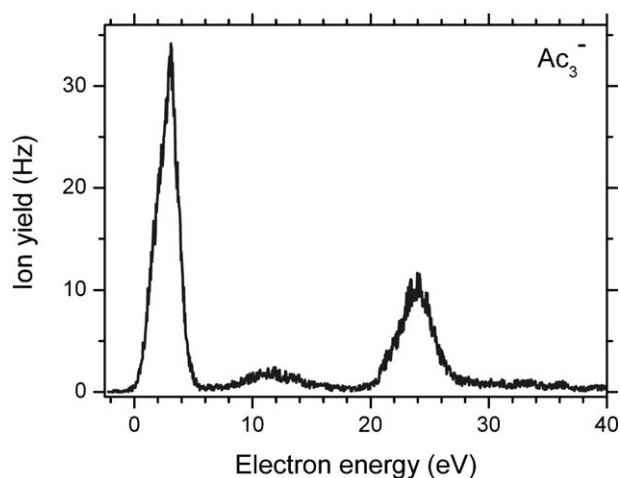


Fig. 5 Yield of the acetic acid trimer anion as a function of electron kinetic energy.

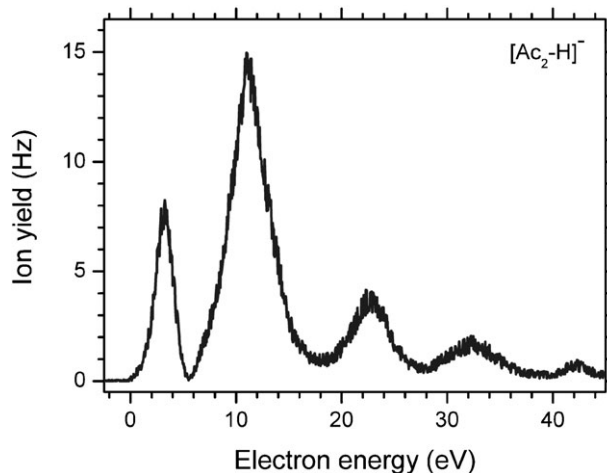


Fig. 6 Yield of the dehydrogenated acetic acid trimer anion as a function of electron kinetic energy.

anions. Quenching by the surrounding helium can funnel these excited anions into the H atom loss channel, reducing the conversion to other fragment anions.<sup>24</sup> This is consistent with the mass spectrometric observation of only minor fragments other than the dehydrogenated parent anion. Confirmation is provided by Fig. 7, which shows the efficiency curves for ejection of H<sub>2</sub>O, OH and O from the dimer anion. The efficiency curves of the latter two are essentially the same as that shown in Fig. 6. Surprisingly, the formation of the acetic anhydride anion is not quenched in the He droplet. Furthermore, the anion efficiency curve differs clearly from H, O and OH loss. Generally, the ratio of the intensity of the low-energy resonance at about 2 eV and the one in combination with inelastic scattering of the electron by a helium atom at about 22 eV is a constant. However, in case of water loss the resonance at about 22 eV is almost twice as large, compared to the other fragments. This indicates that an additional process contributes to H<sub>2</sub>O loss which involves electronic excitation of He. At this energy positive ionization *via* Penning ionization of the dopant is possible and may contribute to the water loss. Thus we propose that electron capture of acetic

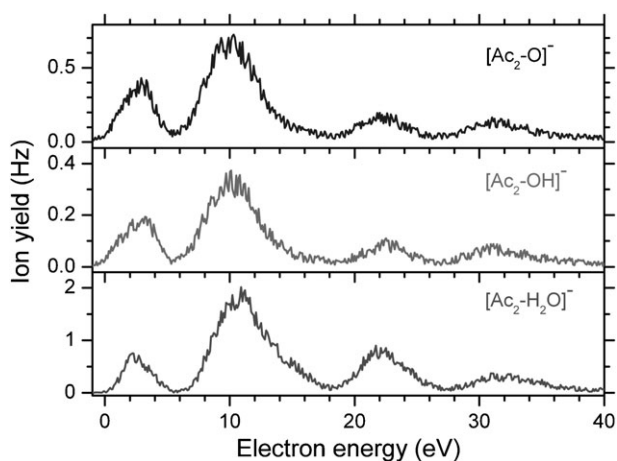


Fig. 7 Ion yields of  $(\text{CH}_3\text{COOH})\text{-(CH}_3\text{COH)}^-$ ,  $(\text{CH}_3\text{COOH})\text{-(CH}_3\text{CO)}^-$  and  $(\text{CH}_3\text{CO})_2\text{O}^-$  as a function of electron energy.

anhydride formed *via* reaction (3), where also two secondary electrons initially are formed, as a possible reaction path. Note also that the lowest energy resonance in Fig. 5–7 is given an artificially low intensity because of enhanced autodetachment from He droplets.<sup>17,23</sup>

#### 4. Conclusions

Electron ionization of helium nanodroplets doped with acetic acid clusters yields the protonated parent species as the dominant product ions. No evidence has been found for the survival of unprotonated parent cations. Another notable product is the species  $\text{Ac}_n\text{H}^+\cdot\text{H}_2\text{O}$ , which is observed only for  $n \geq 5$ . Through the addition of partially deuterated acetic acid, we have shown that this species is a product of an intra-cluster reaction rather than from pick-up of trace water vapour from within the vacuum chambers. This is in marked contrast to the gas phase, where these clusters are formed only by the deliberate addition of water. The reason why these clusters are not seen for  $n < 5$  is currently unknown.

In the case of anion production there is a clear distinction between the monomer and the clusters. For the monomer the dominant product is the dehydrogenated species,  $[\text{Ac-H}]^-$ , whereas for the clusters both the parent anion,  $\text{Ac}_n^-$ , and the dehydrogenated species,  $[\text{Ac}_n\text{-H}]^-$ , have similar abundances. As with the positive ion spectra, there are some marked changes in ion chemistry when compared with the gas phase. In the gas phase  $\text{CH}_2$  elimination is a significant reaction but in helium nanodroplets this process is entirely absent. Removal of  $\text{CH}_2$  most likely requires a loose transition state whose formation is impeded by the surrounding liquid helium. By way of contrast a tight transition state may explain why hydrated anions are seen in the mass spectra as fragmentation products.

Another important difference between the monomer and the cluster anions is the observation of attached helium atoms to the latter but not to the former. Specifically, both  $\text{Ac}_n^-\cdot\text{He}_k$  and  $[\text{Ac}_n\text{-H}]^-\cdot\text{He}_k$  clusters are readily observed for  $n \geq 2$ . We propose that this monomer/cluster disparity arises because of the formation of acyclic (head-to-tail) isomers of acetic acid

clusters in helium nanodroplets, in contrast to the dominant cyclic species formed in the gas phase. The head-to-tail structure is a local minimum on the potential energy surface and clusters are guided into this minimum by long range dipole–dipole steering and become trapped there by the ultra-low temperature of the surrounding matrix. We postulate that the acyclic cluster anions generate much stronger interactions with helium atoms because of their asymmetric charge distributions, and in particular their substantial dipole moments, leading to the survival of anionic clusters with helium atoms attached.

#### Acknowledgements

This work was partially supported by the FWF, P19073, Wien. Some of this work forms part of the ESF network programme EIPAM and EU/ESF RADAM COST Action-P9. S.D. gratefully acknowledges an APART scholarship from the Austrian Academy of Sciences. G.M. and A.M.E. acknowledge ECCL COST Action CM0601 and M.D. acknowledges EIPAM for providing travel funds. S.F.Y. is grateful to the UK EPSRC for the award of an Advanced Fellowship.

#### References

- 1 L. Sanche, *Eur. Phys. J. D*, 2005, **35**, 367–390.
- 2 E. Illenberger and J. Momigny, *Gaseous Molecular Ions. An Introduction to Elementary Processes Induced by Ionization*, Springer, 1992.
- 3 B. Boudaiffa, P. Cloutier, D. Hunting, M. A. Huels and L. Sanche, *Science*, 2000, **287**, 1658–1660.
- 4 W. Sailer, A. Pelc, M. Prost, J. Limtrakul, P. Scheier, E. Illenberger and T. D. Märk, *Chem. Phys. Lett.*, 2003, **378**, 250–256.
- 5 A. Pelc, W. Sailer, P. Scheier and T. D. Märk, *Vacuum*, 2005, **78**, 631–634.
- 6 J. Langer, I. Martin, G. Karwasz and E. Illenberger, *Int. J. Mass Spectrom.*, 2006, **477**, 249–250.
- 7 R. Sievert, I. Cadez, J. Van Doren and A. W. Castleman, Jr, *J. Phys. Chem.*, 1984, **88**, 4502–4505.
- 8 C. Lifshitz and W. Y. Feng, *Int. J. Mass Spectrom. Ion Processes*, 1995, **146–147**, 223–232.
- 9 Y. B. Pithawalla, C. Covington, I. McComish, I. N. Germanenko and M. Samy El-Shall, *Int. J. Mass Spectrom.*, 2002, **218**, 49–62.
- 10 S. Denifl, I. Mähr, F. Ferreira da Silva, F. Zappa, T. D. Märk and P. Scheier, *Eur. Phys. J. D*, 2009, **51**, 73–79.
- 11 H. Schöbel, M. Dampc, F. Ferreira da Silva, A. Mauracher, F. Zappa, S. Denifl, T. D. Märk and P. Scheier, *Int. J. Mass Spectrom.*, 2009, **280**, 26–31.
- 12 S. Jaksch, A. Mauracher, A. Bacher, S. Denifl, F. Ferreira da Silva, H. Schöbel, O. Echt, T. D. Märk, M. Probst, D. K. Bohme and P. Scheier, *J. Chem. Phys.*, 2008, **129**, 224306.
- 13 S. Denifl, F. Zappa, I. Mähr, A. Mauracher, M. Probst, T. D. Märk and P. Scheier, *J. Am. Chem. Soc.*, 2008, **130**, 5065–5071.
- 14 F. Zappa, S. Denifl, I. Mähr, J. Lecointre, F. Rondino, O. Echt, T. D. Märk and P. Scheier, *Eur. Phys. J. D*, 2007, **43**, 117–120.
- 15 S. Feil, K. Gluch, S. Denifl, F. Zappa, O. Echt, P. Scheier and T. D. Märk, *Int. J. Mass Spectrom.*, 2006, **252**, 166–172.
- 16 S. Denifl, M. Stano, A. Stamatovic, P. Scheier and T. D. Märk, *J. Chem. Phys.*, 2006, **124**, 054320.
- 17 S. Denifl, F. Zappa, I. Mähr, J. Lecointre, M. Probst, T. D. Märk and P. Scheier, *Phys. Rev. Lett.*, 2006, **97**, 043201.
- 18 F. Ferreira da Silva, P. Bartl, S. Denifl, O. Echt, T. D. Märk and P. Scheier, *Phys. Chem. Chem. Phys.*, 2009, **11**, 9791.
- 19 J. P. Toennies and A. F. Vilesov, *Angew. Chem., Int. Ed.*, 2004, **43**, 2622–2648.
- 20 F. Stienkemeier and K. Lehman, *J. Phys. B: At., Mol. Opt. Phys.*, 2006, **39**(8), R127–R166.

- 21 A. Scheidemann, B. Schilling and J. P. Toennies, *J. Phys. Chem.*, 1993, **97**, 2128–2138.
- 22 S. Yang, S. M. Brereton, M. D. Wheeler and A. M. Ellis, *J. Phys. Chem. A*, 2006, **110**, 1791–1797.
- 23 A. Mauracher, H. Schöbel, F. Ferreira da Silva, A. Edtbauer, C. Mitterdorfer, S. Denifl, T. D. Märk, E. Illenberger and P. Scheier, *Phys. Chem. Chem. Phys.*, 2009, **11**, 8240.
- 24 S. Denifl, F. Zappa, A. Mauracher, F. Ferreira da Silva, A. Bacher, O. Echt, T. D. Märk, D. K. Böhme and P. Scheier, *ChemPhysChem*, 2008, **9**, 1387–1389.
- 25 F. Zappa, S. Denifl, I. Mähr, A. Bacher, O. Echt, T. D. Märk and P. Scheier, *J. Am. Chem. Soc.*, 2008, **130**, 5573–5578.
- 26 F. Ferreira da Silva, P. Waldburger, S. Jaksch, A. Mauracher, S. Denifl, O. Echt, T. D. Märk and P. Scheier, *Chem.–Eur. J.*, 2009, **15**, 7101–7108.
- 27 E. Coccia, F. Marinetti, E. Bodo and F. A. Gianturco, *J. Chem. Phys.*, 2008, **128**, 134511.
- 28 E. Coccia, F. Marinetti, E. Bodo and F. A. Gianturco, *ChemPhysChem*, 2008, **9**, 1323–1330.
- 29 Y. Marechal, *J. Chem. Phys.*, 1987, **87**, 6344–6353.
- 30 W. Qian and S. Krimm, *J. Phys. Chem.*, 1996, **100**, 14602–14608.
- 31 J. L. Derissen, *J. Mol. Struct.*, 1971, **7**, 67–80.
- 32 C. Riehn, V. V. Matylitsky, M. F. Gelin and B. Brutschy, *Mol. Phys.*, 2005, **103**, 1615–1623.
- 33 S. T. Shipman, P. C. Douglass, H. S. Yoo, C. E. Hinkle, E. L. Mierzejewski and B. H. Pate, *Phys. Chem. Chem. Phys.*, 2007, **9**, 4572–4586.
- 34 F. Madeja, M. Havenith, K. Nauta, R. E. Miller, J. Chocholousova and P. Hobza, *J. Chem. Phys.*, 2004, **120**, 10554–10560.
- 35 M. Gantenberg, M. Halupka and W. Sander, *Chem.–Eur. J.*, 2000, **6**, 1865–1869.
- 36 P. Rodziewicz and N. L. Doltsinis, *J. Phys. Chem. A*, 2009, **113**, 6266–6274.
- 37 O. Dorosh and Z. Kisiel, *Acta Physica Polonica A*, 2007, **312**, S95–S104.
- 38 T. Nakabayashi, H. Sato, F. Hirata and N. Nishi, *J. Phys. Chem. A*, 2001, **105**, 245–250.